ANALYTICAL METHODS OF GENERATING MULTIPLE SOUND ZONES FOR OPEN AND BAFFLED CIRCULAR LOUDSPEAKER ARRAYS

Takuma Okamoto

National Institute of Information and Communications Technology
3-5, Hikaridai, Seika-cho, Soraku-gun, Kyoto, 619-0289, Japan
okamoto@nict.go.jp

ABSTRACT

This paper proposes analytical methods for generating acoustically bright and dark zones on the horizontal plane using circular loudspeaker arrays without and with a cylindrical rigid baffle. Both sound fields on the horizontal plane produced by continuous circular monopole source distributions without and with a rigid baffle are analytically calculated using 2.5D sound field representation derived from the 3D cylindrical harmonics expansion. Efficient spatial filters in the spatial Fourier series domain are analytically derived by modeling sound pressures at the control circle as a rectangular window that corresponds to bright and dark zones. The computer simulation results show that the proposed methods can generate bright and dark zones near the loudspeakers more accurately than conventional least squares and beamforming methods.

Index Terms— Multiple sound zones, personal audio system, circular loudspeaker array, beamforming, cylindrical harmonics expansion

1. INTRODUCTION

Generating acoustically bright and dark zones [1] and multiple sound zones are important and challenging acoustic communication techniques. They are useful not only for personal sound systems [2–8] but also for multilingual guide services and other virtual reality applications. Many methods have been proposed that control both the acoustic contrast and the energy between two spaces [1,3–6,9–14] and reproduce multiple sound fields [8,15–19] using multiple loudspeakers. For realizing personal audio systems and multiple sound zones, these approaches are more effective than beamforming methods [2, 20–22], which maximize the energy to the target direction with the given input source power.

Most existing methods are based on the least squares solution numerically calculated using the control points and the loudspeaker positions [1, 3–6, 11, 17]. Such methods, however, are quite unstable because the acoustic inverse problem is very ill-conditioned [23]. This problem is the same in the least squares based pressure-matching method [24].

Analytical approaches, on the other hand, have been proposed for generating bright and dark zones at arbitrary horizontal positions with arbitrary width using a linear sound source [10, 12]. These methods are based on the spectral division method (SDM) [25], which is a sound field reproduction scheme, and spatial filtering in the wavenumber domain. This method [12] can generate bright and dark zones more efficiently than the conventional energy difference maximization method [9]. However, as sound field reproduction using linear loudspeaker arrays [25, 26], this method is based on the continuous linear distributions of sound sources, and many loudspeakers and a large production space are required.

To generate bright and dark zones using a compact loudspeaker array suited for practical implementations, this paper proposes new analytical methods for open and baffled circular loudspeaker arrays that reduce the number of loudspeakers and the production space.

Pressure-matching and mode-matching beamforming methods using a circular loudspeaker array mounted on a cylindrical rigid baffle have been proposed [20, 21, 27–29]. These methods, however, cannot precisely control sound field near the loudspeakers because the formulations in [27–29] include the far field approximation used in [23] and a horizontal far field is assumed in [20,21]. To control sound field near the loudspeakers effectively, the proposed methods derive analytical solution without far field approximation. Moreover, they can control sound field using an open circular loudspeaker array (without a baffle) suited to be combined with visual applications.

The proposed methods are based on 2.5D sound field representation [25, 30] analytically derived from the 3D cylindrical harmonics expansion [23] for a continuous circular sound source, and bright and dark zones are generated outside a circular source on the horizontal plane. Firstly, both sound fields on the horizontal plane produced by continuous circular sound sources without and with a cylindrical baffle are analytically derived. After that, as a method based on SDM using a linear sound source [12], efficient spatial filters in the spatial Fourier series domain are also analytically derived by modeling sound pressures at the control circle as a rectangular window that corresponds to bright and dark zones.

2. 2.5D SOUND FIELD REPRESENTATION FOR CONTINUOUS CIRCULAR MONOPOLE SOURCE DISTRIBUTIONS

For actual implementations, sound field reproduction systems are frequently simplified to be reproduced in the horizontal plane. Then the secondary sources are arranged on a line or a circle. In actual implementations, monopole sources instead of line sources are usually employed for secondary sources. Such approaches are called 2.5D sound field reproduction [25, 30]. In this section, 2.5D sound representation for continuous circular sound sources on the horizontal plane is analytically derived from the 3D cylindrical harmonics expansion.

This study was partly supported by JSPS KAKENHI Grant Numbers 25871208 and 15K21674.

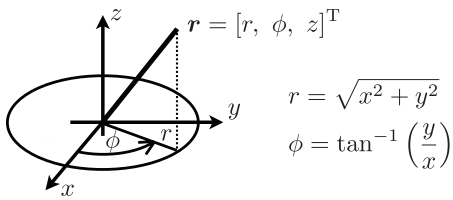

Figure 1: Definition of cylindrical coordinates $\boldsymbol{r} = [r,\ \phi,\ z]^{\mathrm{T}}$ relative to Cartesian coordinates $\boldsymbol{x} = [x,\ y,\ z]^{\mathrm{T}}$.

2.1. Sound field due to a cylindrical sound source

To describe precise horizontal sound field produced by a continuous circular monopole source distribution, the sound field produced by a continuous cylindrical sound source is introduced as in [31].

As in [23], cylindrical coordinates $\boldsymbol{r} = [r,\ \phi,\ z]^{\mathrm{T}}$ relative to Cartesian coordinates $\boldsymbol{x} = [x,\ y,\ z]^{\mathrm{T}}$ are defined in Fig. 1. As in [31,32], the sound pressure $P(\boldsymbol{r}, \omega)$ synthesized at position $\boldsymbol{r} = [r,\ \phi,\ z]^{\mathrm{T}}$ by a continuous cylindrical sound source with radius r_0 is given as

$$P(\boldsymbol{r}, \omega) = \int_0^{2\pi}\int_{-\infty}^{\infty} D(\boldsymbol{r}_0, \omega) G(\boldsymbol{r}, \boldsymbol{r}_0, \omega) r_0 dz_0 d\phi_0, \quad (1)$$

where $\omega = 2\pi f$ denotes the radial frequency, f represents the temporal frequency, $D(\boldsymbol{r}_0, \omega)$ stands for the driving function of a cylindrical sound source at $\boldsymbol{r}_0 = [r_0,\ \phi_0,\ z_0]^{\mathrm{T}}$ and $G(\boldsymbol{r}, \boldsymbol{r}_0, \omega)$ is the transfer function from a sound source position $\boldsymbol{r}_0$ to a receiver position $\boldsymbol{r}$.

2.2. Sound field due to a cylindrical source without a baffle

When a continuous cylindrical sound source is assumed to be acoustically transparent and under the free-field assumption, $G(\boldsymbol{r}, \boldsymbol{r}_0, \omega)$ in (1) is the three-dimensional free-field Green's function [23].

When $r > r_0$, using the two-dimensional spatial Fourier transform of the three-dimensional free-field Green's function with respect to ϕ and z derived in [23, 31], the 3D cylindrical harmonics expansion of $G(\boldsymbol{r}, \boldsymbol{r}_0, \omega)$ is represented as

$$G_{\mathrm{open}}(\boldsymbol{r}, \boldsymbol{r}_0, \omega) = \frac{e^{jk|\boldsymbol{r}-\boldsymbol{r}_0|}}{4\pi|\boldsymbol{r}-\boldsymbol{r}_0|} \quad (2)$$

$$= \sum_{n=-\infty}^{\infty} \frac{1}{2\pi} \int_{-\infty}^{\infty} \frac{j}{4} J_n(k_r r_0) H_n^{(1)}(k_r r) e^{jn(\phi-\phi_0)} e^{jk_z(z-z_0)} dk_z, \quad (3)$$

where $j = \sqrt{-1}$, $k = \omega/c$, $H_n^{(1)}$ and J_n denote the wavenumber, the n-th order Hankel function of the first kind and the n-th order Bessel function of the first kind, respectively [23]. c is the speed of sound and $k_r = \sqrt{k^2 - k_z^2}$.

2.3. Sound field due to a cylindrical source with a rigid baffle

In the proposed method, a continuous circular sound source mounted on the surface of a cylindrical rigid baffle with radius r_0 and infinite length to the z-axis is assumed as in [20]. In [20], however, sound field on the horizontal plane due to a continuous circular source ($z = 0$) was only considered with the far field assumption. When a continuous circular monopole source distribution is assumed, precise representation of three-dimensional sound field must be required for describing sound field on the horizontal plane as conventional 2.5D sound field reproduction methods [25, 30]. In this subsection, the 3D cylindrical harmonics expansion of the transfer function $G_{\mathrm{baffled}}(\boldsymbol{r}, \boldsymbol{r}_0, \omega)$ from a sound source mounted on a rigid cylinder $\boldsymbol{r}_0$ to a receiver $\boldsymbol{r}(r > r_0)$ is analytically derived.

As in [23, 32], given a rigid cylinder of radius r_0, the incident field $P_{\mathrm{i}}(\boldsymbol{r}, \omega)$ and scattered field $P_{\mathrm{s}}(\boldsymbol{r}, \omega)$ are respectively described as

$$P_{\mathrm{i}}(\boldsymbol{r}, \omega) = \sum_{n=-\infty}^{\infty} \frac{1}{2\pi} \int_{-\infty}^{\infty} C_n(k_z, \omega) J_n(k_r r) e^{jn\phi} e^{jk_z z} dk_z, \quad (4)$$

$$P_{\mathrm{s}}(\boldsymbol{r}, \omega) = \sum_{n=-\infty}^{\infty} \frac{1}{2\pi} \int_{-\infty}^{\infty} A_n(k_z, \omega) H_n^{(1)}(k_r r) e^{jn\phi} e^{jk_z z} dk_z, \quad (5)$$

where $C_n(k_z, \omega)$ and $A_n(k_z, \omega)$ are coefficients that depend on the incident field. The sound pressure gradient on the surface of the rigid baffle with radius r_0 becomes zero and the relation $A_n(k_z, \omega) = -J_n'(k_r r_0) C_n(k_z, \omega) / H_n^{(1)\prime}(k_r r_0)$, is obtained as in [32], where J_n' and $H_n^{(1)\prime}$ are the derivatives of J_n and $H_n^{(1)}$, respectively. If $r = r_0$, the total sound field $P(\boldsymbol{r}, \omega) = P_{\mathrm{i}}(\boldsymbol{r}, \omega) + P_{\mathrm{s}}(\boldsymbol{r}, \omega)$ is given by the sum of the incident and scattered fields as

$$P(\boldsymbol{r}_0, \omega) = \sum_{n=-\infty}^{\infty} \frac{1}{2\pi} \int_{-\infty}^{\infty} \frac{2jC_n(k_z, \omega)}{\pi k_r r_0 H_n^{(1)\prime}(k_r r_0)} e^{jn\phi_0} e^{jk_z z_0} dk_z. \quad (6)$$

Whereas a plane wave is impinged in [20], for the case of a spherical wave impinging from $\boldsymbol{r}$ $(r > r_0)$, the incident sound field $P_{\mathrm{i}}(\boldsymbol{r}_0, \omega)$ is obtained from (3) and represented as

$$P_{\mathrm{i}}(\boldsymbol{r}_0, \omega) = \frac{e^{jk|\boldsymbol{r}_0-\boldsymbol{r}|}}{4\pi|\boldsymbol{r}_0-\boldsymbol{r}|}$$

$$= \sum_{n=-\infty}^{\infty} \frac{1}{2\pi} \int_{-\infty}^{\infty} \frac{j}{4} J_n(k_r r_0) H_n^{(1)}(k_r r) e^{jn(\phi_0-\phi)} e^{jk_z(z_0-z)} dk_z. \quad (7)$$

From (4) and (7), $C_n(k_z, \omega) = (j/4) H_n^{(1)}(k_r r) e^{-jn\phi} e^{-jk_z z}$. Finally, using the principle of reciprocity between source and receiver as in [20], the 3D cylindrical harmonics expansion of the transfer function $G_{\mathrm{baffled}}(\boldsymbol{r}, \boldsymbol{r}_0, \omega)$ from a sound source on a rigid cylinder $\boldsymbol{r}_0$ to a receiver $\boldsymbol{r}(r > r_0)$ is analytically derived from (6) and given as

$$G_{\mathrm{baffled}}(\boldsymbol{r}, \boldsymbol{r}_0, \omega)$$

$$= \sum_{n=-\infty}^{\infty} \frac{1}{2\pi} \int_{-\infty}^{\infty} \frac{-H_n^{(1)}(k_r r)}{2\pi k_r r_0 H_n^{(1)\prime}(k_r r_0)} e^{jn(\phi-\phi_0)} e^{jk_z(z-z_0)} dk_z. \quad (8)$$

2.4. 2.5D sound field representation for continuous circular sound sources without and with a rigid baffle

Sound pressure $P(\boldsymbol{r}, \omega)$ synthesized at position $\boldsymbol{r}$ by a continuous circular monopole source distribution with radius r_0 centered at the origin on the x-y plane (Fig. 2) is also given as

$$P(\boldsymbol{r},\omega) = \int_0^{2\pi} D(r_0,\phi_0,z=0,\omega)G(\boldsymbol{r},\boldsymbol{r}_0,\omega)r_0 d\phi_0. \quad (9)$$

Just as in [30], when the spatial Fourier series expansion [23] is applied to (9) with $z=0$, the circular convolution theorem holds and the driving function of a circular sound source is directly derived as

$$\mathring{D}_n(r_0,\omega) = \frac{\mathring{P}_n(r,\omega)}{2\pi r_0 \mathring{G}_n(r,r_0,\omega)}. \quad (10)$$

As in [30], the Fourier series coefficient functions of the horizontal transfer function from a circular sound source with radius r_0 to a reference circle r is analytically derived. For both cases of circular sound sources without and with a cylindrical rigid baffle, $\mathring{G}_{\mathrm{open},n}(r>r_0,\omega)$ and $\mathring{G}_{\mathrm{baffled},n}(r>r_0,\omega)$ are derived from $G_{\mathrm{open}}(r,r_0,\phi,\phi_0,z=z_0=0,\omega)$ in (3) and $G_{\mathrm{baffled}}(r,r_0,\phi,\phi_0,z=z_0=0,\omega)$ in (8), and given as

$$\mathring{G}_{\mathrm{open},n}(r>r_0,\omega) = \frac{1}{2\pi}\int_{-\infty}^{\infty} \frac{j}{4} J_n(k_r r_0) H_n^{(1)}(k_r r) dk_z, \quad (11)$$

$$\mathring{G}_{\mathrm{baffled},n}(r>r_0,\omega) = \frac{1}{2\pi}\int_{-\infty}^{\infty} \frac{-H_n^{(1)}(k_r r)}{2\pi k_r r_0 H_n^{(1)\prime}(k_r r_0)} dk_z. \quad (12)$$

These transfer functions can precisely describe horizontal sound fields produced by continuous circular monopole source distributions without and with a rigid baffle.

3. GENERATION OF MULTIPLE SOUND ZONES USING A CIRCULAR SOUND SOURCE

3.1. Spatial filter modeling

For producing the sound signal $S(\omega)$ at a zone using a circular source, optimal filter $F(\boldsymbol{r}_0,\omega)$ of a circular source is derived here. The sound source driving function is then given as $D(\boldsymbol{r}_0,\omega) = S(\omega)F(\boldsymbol{r}_0,\omega)$. $S(\omega)$ is independent on $F(\boldsymbol{r}_0,\omega)$ and set to 1. In the proposed method, bright and dark zones are generated outside a circular source on the horizontal plane. Then $D(\boldsymbol{r}_0,\omega) = F(\boldsymbol{r}_0,\omega)$, and $\mathring{F}_n(r_0,\omega) = \mathring{P}_n(r,\omega)/2\pi r_0 \mathring{G}_n(r>r_0,\omega)$.

As the SDM-based method [10,12], to generate bright and dark zones at continuous receiver circle $r=r_{\mathrm{ref}}$ on the x-y plane, $P(r_{\mathrm{ref}},\phi,0,\omega)$ is also continuously set to 1 or 0 at all the temporal frequencies. The positions at $P(\boldsymbol{r},\omega)=1$ and 0 correspond to the bright and dark points, respectively. For generating the bright zone of width Φ centered around $\phi=\phi_{\mathrm{S}}$ at $r=r_{\mathrm{ref}}$ as shown in Fig. 2, $P(r,\phi,0,\omega)$ is also modeled by a rectangular window and given as

$$P(r_{\mathrm{ref}},\phi,0,\omega) = \begin{cases} 1, & \text{for} \quad \phi_{\mathrm{S}}-\Phi/2 \le \phi \le \phi_{\mathrm{S}}+\Phi/2 \\ 0, & \text{elsewhere.} \end{cases} \quad (13)$$

The spatial Fourier series expansion is applied to (13) with respect to ϕ, described as a sinc function [23], and represented as

$$\mathring{P}_n(\Phi,\phi_{\mathrm{S}},\omega) = \Phi \mathrm{sinc}\left(\frac{n\Phi}{2\pi}\right) e^{-jn\phi_{\mathrm{s}}}. \quad (14)$$

The spatial filter in the spatial Fourier series domain for generating bright and dark zones is then analytically derived as

$$\mathring{F}_n(r_0,r_{\mathrm{ref}},\Phi,\phi_{\mathrm{s}},\omega) = \frac{\Phi \mathrm{sinc}(n\Phi/2\pi)e^{-jn\phi_{\mathrm{s}}}}{2\pi r_0 \mathring{G}_n(r_{\mathrm{ref}}>r_0,\omega)}. \quad (15)$$

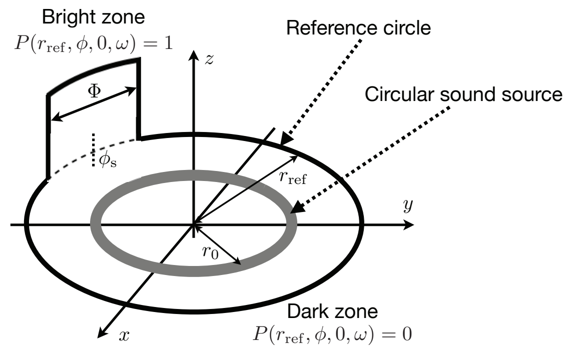

Figure 2: Produced sound pressure $P(r_{\mathrm{ref}},\phi,0,\omega)$ modeled by rectangular window at r_{ref} centered ϕ_{s} with width Φ.

Consequently, similar to the SDM-based method [12], a bright zone of arbitrary width Φ can be generated at arbitrary horizontal direction ϕ_{s} with $r_{\mathrm{ref}} > r_0$ by the proposed spatial filter in spatial Fourier series domain $\mathring{F}_n(r_0,r_{\mathrm{ref}},\Phi,\phi_{\mathrm{s}},\omega)$ using a continuous circular monopole source distribution.

3.2. Actual implementation using a circular loudspeaker array

For an actual implementation, a circular loudspeaker array instead of a continuous circular source is used and (15) must be discretized. When the number of loudspeakers is L and the array's radius is r_0, the order n of the spatial Fourier series in (15) can be calculated up to $N=\lfloor (L-1)/2 \rfloor$, where $\lfloor\cdot\rfloor$ is the floor function. However, the spatial Fourier series at $|n|>|kr_0|$ is the evanescent component and is quite large because of the inverse propagation when $r_{\mathrm{ref}} > r_0$ [23]. To calculate a stable filter, n is up to $N=\lfloor |kr_0| \rfloor$ if $\lfloor |kr_0| \rfloor < \lfloor (L-1)/2 \rfloor$. Finally, the filter coefficient of each loudspeaker at ϕ_l in the temporal frequency domain is obtained as

$$F(r_0,\phi_l,\omega) = \sum_{n=-N}^{N} \mathring{F}_n(r_0,\omega)e^{jn\phi_l}, \quad l=1,2,\cdots L. \quad (16)$$

The proposed methods can be realized by fewer loudspaekers than in the SDM-based method using a linear loudspeaker array [12] if the circular array's radius is small.

4. EXPERIMENTS

Computer simulations were performed to evaluate the proposed methods compared with conventional least squares (LS) based pressure-matching methods [24] and beamforming (BF) methods using circular loudspeaker arrays with and without a rigid baffle.

For the case of a circular array mounted on a rigid baffle, the analytical beamforming solution proposed in [20] was used and combined with the spatial filtering in (14) and given as

$$F_{\mathrm{BF,baffled}}(r_0,\phi_l,\omega) = \sum_{n=-N}^{N} \frac{kr_0 H_n'(kr_0)\Phi \mathrm{sinc}(n\Phi/2\pi)e^{jn(\phi_l-\phi_{\mathrm{s}})}}{4j^{(1-n)}}. \quad (17)$$

$C_n(k_z,\omega) = j^{-n}e^{-jn\phi_{\mathrm{s}}}$ as in [20] and $k_z=0$ in (4), the beamforming filter combined with the spatial filtering in (14) for an open

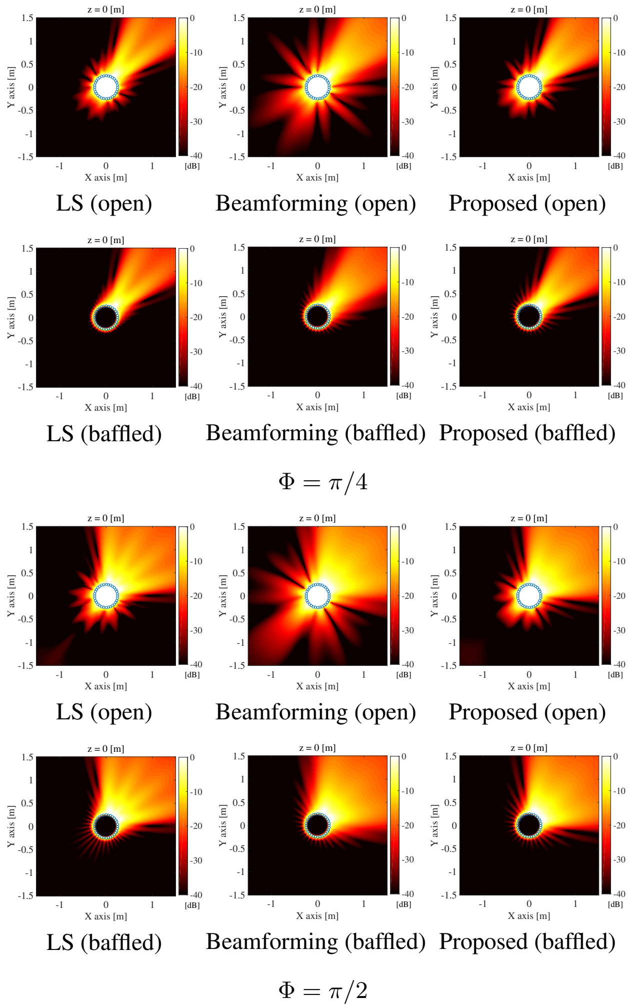

Figure 3: Results of produced sound pressure level with $r_0 = 0.25$ m, $f = 3$ kHz, $\phi_\mathrm{s} = \pi/4$ and $r_\mathrm{ref} = 1.0$ m. Blue circles are loudspeakers with $L = 32$. Sound pressure level at $\boldsymbol{r} = [r_0 + 0.1,\ \phi_\mathrm{s},\ 0]^\mathrm{T}$ is set to 0 dB.

circular array is also analytically derived as

$$F_{\mathrm{BF,open}}(r_0, \phi_l, \omega) = \sum_{n=-N}^{N} \frac{\Phi \mathrm{sinc}(n\Phi/2\pi) e^{jn(\phi_l - \phi_\mathrm{S})}}{2\pi j^{-n} J_n(kr_0)}. \quad (18)$$

In all the calculations, a three-dimensional free field was assumed. The speed of sound c was 343.36 m/s. (8), (11) and (12) were discretized as $dk_z \to \Delta k_z = 0.01$ and truncated as $-100 \leq k_z \leq 100$. A circular loudspeaker array with radius $r_0 = 0.25$ m was centered at the origin and located on the x-y plane. The number of loudspeakers L was 32, which is half of previous experiments [12]. The reference circle's radius for the proposed methods was set to $r_\mathrm{ref} = 1.0$ m. 32 control points were set on r_ref for the LS methods. $F_\mathrm{LS,open}$ and $F_\mathrm{LS,baffled}$ were calculated using (2) and (8) in which n was also truncated within ± 20, respectively.

Similar to the previous work [12], for evaluating the sound pressure level $20\log_{10}|P(\boldsymbol{r}, \omega)|$ between bright zone $\boldsymbol{r}_\mathrm{b}$ and dark zone

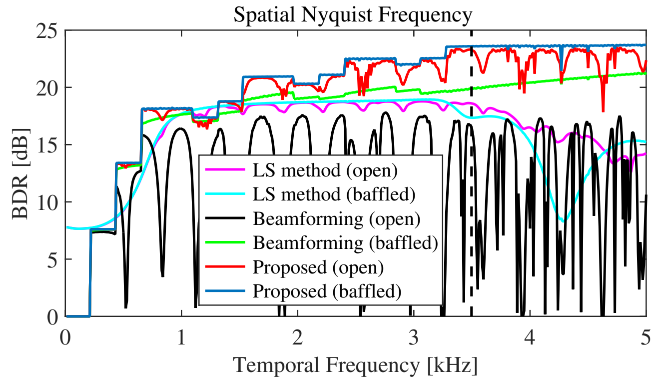

Figure 4: Experimental results of bright to dark ratio $BDR(\omega)$ defined in (19) with $\Phi_\mathrm{b} = \pi/2$ and $\Phi_\mathrm{d} = 3\pi/2$.

$\boldsymbol{r}_\mathrm{d}$, the bright to dark ratio $BDR(\omega)$ was also defined as

$$BDR(\omega) = 20\log_{10} \frac{\sum_{\boldsymbol{r}_\mathrm{b}} |P(\boldsymbol{r}_\mathrm{b}, \omega)| / \Phi_\mathrm{b}}{\sum_{\boldsymbol{r}_\mathrm{d}} |P(\boldsymbol{r}_\mathrm{d}, \omega)| / \Phi_\mathrm{d}}, \quad (19)$$

where Φ_b and Φ_b are the widths of the bright and dark zones, respectively. For calculating (19), both were set around control circle $r_\mathrm{ref} - 0.2 \leq r \leq r_\mathrm{ref} + 0.2$, the bright zone's width was $\Phi_\mathrm{b} = \pi/2$, and the dark zone's width was $\Phi_\mathrm{d} = 3\pi/2$.

Fig. 3 shows the results of each sound pressure level produced by conventional LS, beamforming and proposed methods for $f = 3$ kHz and $\phi_\mathrm{s} = \pi/4$, with $\Phi = \pi/4$ and $\pi/2$, respectively. The result of bright to dark ratio $BDR(\omega)$ with $\Phi = \pi/2$ is depicted in Fig. 4. These results indicate that both proposed methods generate bright and dark zones more accurately than conventional LS and beamforming methods. Moreover, it is obvious that the $BDR(\omega)$ result for the beamforming method using an open circular array is quite unstable at forbidden frequencies where $J_n(kr_0) = 0$ [23]. The proposed method for an open circular array, on the other hand, introduces (11) based on 2.5D sound field representation instead of $J_m(kr_0)$. The $BDR(\omega)$ result, however, suggests that the forbidden frequencies are not a problem in the proposed method for an open circular array. Detailed analysis and discussion are required as future work.

Consequently, the proposed spatial filtering based on 2.5D sound field representation can efficiently control sound pressure near the loudspeakers than conventional least squares and beamforming methods. The transfer functions derived in (11) and (12) can also expect to be efficiently used for sound field reproduction using circular loudspeaker arrays without and with a rigid baffle.

5. CONCLUSION

This paper proposed analytical methods to generate acoustically bright and dark zones on the horizontal plane using circular sound sources without and with a rigid baffle. The spatial filters in the Fourier series domain were analytically derived by introducing 2.5D sound field representation for circular monopole source distributions. The proposed methods can be realized by fewer loudspeakers than in the SDM-based method for a linear array. The computer simulation results show that the proposed methods generate bright and dark zones near the loudspeakers more accurately than conventional least squares and beamforming methods.

6. REFERENCES

[1] J.-W. Choi and Y.-H. Kim, "Generation of an acoustically bright zone with an illuminated region using multiple sources," *J. Acoust. Soc. Am.*, vol. 111, no. 4, pp. 1695–1700, Apr. 2002.

[2] W. F. Druyvesteyn and J. Garas, "Personal sound," *J. Audio Eng. Soc.*, vol. 45, no. 9, pp. 685–701, Sept. 1997.

[3] J.-H. Chang, C.-H. Lee, J.-Y. Park, and Y.-H. Kim, "A realization of sound focused personal audio system using acoustic contrast control," *J. Acoust. Soc. Am.*, vol. 125, no. 4, pp. 2091–2097, Apr. 2009.

[4] S. J. Elliott, J. Cheer, J.-W. Choi, and Y. Kim, "Robustness and regularization of personal audio systems," *IEEE Trans. Audio, Speech, Lang. Process.*, vol. 20, no. 7, pp. 2123–2133, Sept. 2012.

[5] Y. Cai, M. Wu, and J. Yang, "Sound reproduction in personal audio systems using the least-squares approach with acoustic contrast control constraint," *J. Acoust. Soc. Am.*, vol. 135, no. 2, pp. 734–741, Feb. 2014.

[6] P. Coleman, P. J. B. Jackson, M. Olik, and J. A. Pedersen, "Personal audio with a planar bright zone," *J. Acoust. Soc. Am.*, vol. 136, no. 4, pp. 1725–1735, Oct. 2014.

[7] T. Betlehem, W. Zhang, M. Poletti, and T. Abhayapala, "Personal sound zones: Delivering interface-free audio to multiple listeners," *IEEE Signal Process. Mag.*, vol. 32, no. 2, pp. 81–91, Mar. 2015.

[8] M. A. Poletti and F. M. Fazi, "An approach to generating two zones of silence with application to personal sound systems," *J. Acoust. Soc. Am.*, vol. 137, no. 2, pp. 598–605, Feb. 2015.

[9] M. Shin, S. Q. Lee, F. M. Fazi, P. A. Nelson, D. Kim, S. Wang, K. H. Park, and J. Seo, "Maximization of acoustic energy difference between two spaces," *J. Acoust. Soc. Am.*, vol. 128, no. 1, pp. 121–131, July 2010.

[10] K. Helwani, S. Spors, and H. Buchner, "Spatio-temporal signal preprocessing for multichannel acoutic echo cancellation," in *Proc. ICASSP*, May 2011, pp. 93–96.

[11] P. Coleman, P. J. B. Jackson, M. Olik, M. Møller, M. Olsen, and J. A. Pedersen, "Acoustic contrast, planarity and robustness of sound zone methods using a circular loudspeaker array," *J. Acoust. Soc. Am.*, vol. 135, no. 4, pp. 1929–1940, Apr. 2014.

[12] T. Okamoto, "Generation of multiple sound zones by spatial filtering in wavenumber domain using a linear array of loudspeakers," in *Proc. ICASSP*, May 2014, pp. 4733–4737.

[13] M. Shin, F. M. Fazi, P. A. Nelson, and F. C. Hirono, "Controlled sound field with a dual layer loudspeaker array," *J. Sound Vib.*, vol. 333, no. 16, pp. 3794–3817, Aug. 2014.

[14] S. Zhao and X. Qiu, "Acoustic contrast control in an arc-shaped area using a linear loudspeaker array," *J. Acoust. Soc. Am.*, vol. 137, no. 2, pp. 1036–1039, Feb. 2015.

[15] M. Poletti, "An investigation of 2D multizone surround sound systems," in *Proc. 125th Conv. Audio Eng. Soc.*, Oct. 2008.

[16] Y. J. Wu and T. D. Abhayapala, "Spatial multizone soundfield reproduction: theory and design," *IEEE Trans. Audio, Speech, Lang. Process.*, vol. 19, no. 6, pp. 1711–1720, Aug. 2011.

[17] N. Radmanesh and I. S. Burnett, "Generation of isolated wideband sound fields using a combined two-stage Lasso-LS algorithm," *IEEE Trans. Audio, Speech, Lang. Process.*, vol. 21, no. 2, pp. 378–387, Feb. 2013.

[18] W. Jin, W. B. Kleijn, and D. Virette, "Multizone soundfield reproduction using orthogonal basis expansion," in *Proc. ICASSP*, May 2013, pp. 311–315.

[19] W. Jin and W. B. Kleijn, "Multizone soundfield reproduction in reverberant rooms using compressed sensing techniques," in *Proc. ICASSP*, May 2014, pp. 4728–4732.

[20] F. M. Fazi, M. Shin, F. Olivieri, S. Fontana, and L. Yue, "Comparison of pressure-matching and mode-matching beamforming methods for circular loudspeaker arrays," in *Proc. 137th Conv. Audio Eng. Soc.*, Oct. 2014.

[21] F. M. Fazi, M. Shin, F. Olivieri, and S. Fontana, "Low frequency performance of circular loudspeaker arrays," in *Proc. 138th Conv. Audio Eng. Soc.*, May 2015.

[22] M. R. Bai and Y.-H. Hsieh, "Point focusing using loudspeaker arrays from the perspective of optimal beamforming," *J. Acoust. Soc. Am.*, vol. 137, no. 6, pp. 3393–3410, June 2015.

[23] E. G. Williams, *Fourier Acoustics: Sound Radiation and Nearfield Acoustic Holography*. London, UK: Academic Press, 1999.

[24] T. Betlehem and T. D. Abhayapala, "Theory and design of sound field reproduction in reverberant rooms," *J. Acoust. Soc. Am.*, vol. 117, no. 4, pp. 2100–2111, Apr. 2005.

[25] J. Ahrens and S. Spors, "Sound field reproduction using planar and linear arrays of loudspeakers," *IEEE Trans. Audio, Speech, Lang. Process.*, vol. 18, no. 8, pp. 2038–2050, Nov. 2010.

[26] T. Okamoto, S. Enomoto, and R. Nishimura, "Least squares approach in wavenumber domain for sound field recording and reproduction using multiple parallel linear arrays," *Appl. Acoust.*, vol. 86, pp. 95–103, Dec. 2014.

[27] M. Kolundžija, C. Faller, and M. Vetterli, "Baffled circular loudspeaker array with broadband high directivity," in *Proc. ICASSP*, Mar. 2010, pp. 73–76.

[28] ——, "Design of a compact cylindrical loudspeaker array for spatial sound reproduction," in *Proc. 130th Conv. Audio Eng. Soc.*, May 2011.

[29] M. Poletti and T. Betlehen, "Design of a prototype variable directivity loudspeaker for improved surround sound reproduction in rooms," in *Proc. 52nd Int. Conf. Audio Eng. Soc.*, Sept. 2013.

[30] J. Ahrens and S. Spors, "An analytical approach to sound field reproduction using circular and spherical loudspeaker distributions," *Acta Acust. Utd. With Acust.*, vol. 94, no. 6, pp. 988–999, Nov./Dec. 2008.

[31] T. Okamoto, "Near-field sound propagation based on a circular and linear array combination," in *Proc. ICASSP*, Apr. 2015, pp. 624–628.

[32] S. Koyama, K. Furuya, Y. Hiwasaki, Y. Haneda, and Y. Suzuki, "Wave field reconstruction filtering in cylindrical harmonic domain for with-hight recording and reproduction," *IEEE/ACM Trans. Audio, Speech, Lang. Process.*, vol. 22, no. 10, pp. 1546–1557, Oct. 2014.